JOURNAL OF MATERIALS SCIENCE **36** (2001) 3189–3195

Improved contacting by the use of silver in solid oxide fuel cells up to an operating temperature of 800 °C

W. A. MEULENBERG
Forschungszentrum Jülich GmbH, Institute for Materials and Processes in Energy Systems, IWV-1, D-52425 Jülich, Germany
E-mail: w.a.meulenberg@fz-juelich.de

O. TELLER
Forschungszentrum Jülich GmbH, Institute for Materials and Processes in Energy Systems, IWV-2, D-52425 Jülich, Germany

U. FLESCH, H. P. BUCHKREMER, D. STÖVER
Forschungszentrum Jülich GmbH, Institute for Materials and Processes in Energy Systems, IWV-1, D-52425 Jülich, Germany

In the following, a contacting variant for solid oxide fuel cells will be presented in which the conductivity of the interconnect is ensured by contact elements made of fine silver. To this end, the interconnect has holes through which the contact elements of fine silver (99.9 wt% Ag) are introduced and then pressed. This pressing process and the thermal expansion of the silver during heating leads to a gastight joint. The silver penetrations are additionally soldered to render them capable of withstanding temperature cycling. Contact resistance measurements and corrosion studies at 800 °C in air or Ar/4 vol.% H_2/3 vol.% H_2O demonstrate the functionality of the contacting variant under the described conditions. The experimental results indicate that contacting by means of silver contact elements ensures long-term stability up to operating temperatures of 800 °C. Current transmission via the silver contact elements means that a large number of materials are conceivable as the interconnect material. In the following application, an FeCrAl steel (1.4767, Aluchrom Y Hf—trade name Krupp Thyssen Nirosta) with 5.7 wt.% aluminium was used. At the operating temperature, a dense aluminium oxide layer forms on its surface which prevents the vaporization, for example of chromium oxide species, during fuel cell operation.

1. Introduction

A fuel cell's mode of operation is based on a direct conversion of chemical energy into electrical energy. There is no combustion process such as that which precedes the generation of energy in heat engines. A more efficient and environmentally acceptable use of energy resources is possible due to the direct conversion of energy. Combustion involves great energy losses since the energy of the fuel is first transformed into heat and then into electrical energy via a generator. The high-temperature fuel cell has an oxygen-ion-conducting solid electrolyte, an anode and a cathode—the integrated system being termed the membrane electrode assembly (MEA). Good electrical conductivity between the electrodes and the interconnect requires good contacting between the individual components in the fuel cell stack so that a sufficient number of contact points must be present at which the formation of electrically insulating corrosion products can be practically ruled out. The element silver enables good contacting up to an operating temperature of 800 °C. In spite of a weight loss due to vaporization, its good electrical conductivity at the operating temperature remains stable in the long term.

2. State of the art

The so-called anode-supported substrate concept in which electrolyte and cathode are applied onto a Ni/ZrO_2 anode 1.5 mm in thickness was developed at Research Centre Jülich [1]. In order to ensure improved contact between the interconnect material and the electrodes, a nickel mesh was additionally employed on the anode side. On the cathode side, a cathode function layer applied onto the interconnect ensures improved contacting. Stainless steels containing chromium were used as the interconnect material (e.g. 1.4742) [2]. The gas was supplied via channels milled into the interconnect.

3. Experimental

3.1. Fabricating the silver pin interconnects and experimental procedure

In this contacting variant, the interconnects of FeCrAl (Aluchrom Y Hf) are equipped with fine-silver rivet heads and after pressing the heads of the contact elements project several centimetres on both sides of the sheet. After holes have been made in the interconnect corresponding to the shank diameter of the rivet heads, the silver pins are inserted through the sheet and then pressed at room temperature. If this pressing process is, for example, performed by a uniaxial press then uniform pressing is achieved thus ensuring that all rivet heads display uniform height. A gastight joint between the interconnect and rivet head is achieved by pressing the silver and due to the high thermal expansion during heating ($\alpha = 18.9 \cdot 10^{-6}$ K^{-1}, [3]). The rivet heads are additionally soldered to ensure that the joint between the silver and interconnect also remains gastight during thermal cycling. Fig. 2 shows the top surface of an interconnect sheet equipped with silver rivet heads for the experiments.

Fig. 3 shows an example of how fine silver is used for contacting in a fuel cell stack.

In contradistinction to Fig. 1, Fig. 3 shows a contacting variant where the current is conducted via silver contact elements passing through a bulk interconnect. The silver rivet heads are distributed uniformly across the surface at intervals of e.g. 1 cm. Due to the limited transverse conductivity of the cathode, a silver mesh is additionally located between the cathode and interconnect. The anode side is equipped with a Ni mesh for contacting purposes. Due to their plastic properties, the two meshes additionally lead to tolerance levelling among the other stack components.

In this contacting variant, the formation of insulating corrosion products at the metallic interconnect can be tolerated since the silver pins ensure the flow of electrical current. The use of ceramic interconnect materials can also be taken into consideration for this contacting variant. The thermal expansion coefficient of the silver should, if possible, be greater than that of the interconnect in order to additionally seal the pin joints during heating. The vaporization rate of the silver contact elements is kept low due to the small area of their surface exposed to the gas flow. A suitable arrangement and size of the silver pins means that additional gas channels can be dispensed with.

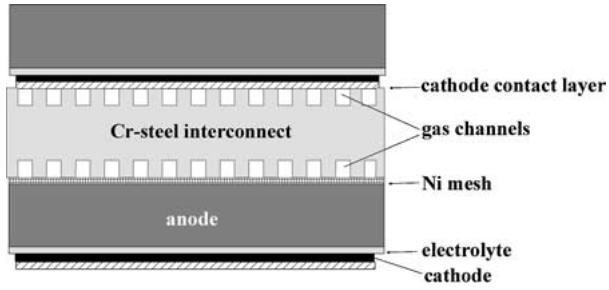

Figure 1 Contacting of a solid oxide fuel cell with a standard interconnect made of a chromium stainless steel with the cathode contact layer.

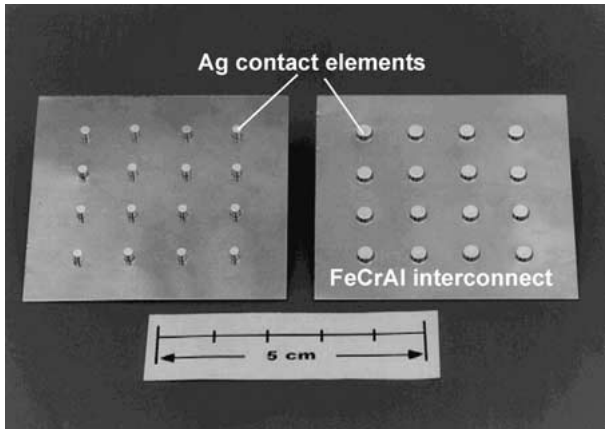

Figure 2 Interconnect foil of FeCrAl with silver contact elements inserted into it before (left) and after (right) pressing.

3.2. Contact resistance measurements

The contact resistance was determined by four-wire technique under operating conditions at 800 °C for a service life of 500 hours. Fig. 4 shows the experimental setup of the measuring assemblies where the voltage drop was read off between points 1 and 2.

Measurements at the anode material were performed under an Ar/4 vol.% H_2/H_2O atmosphere with approx. 3 vol.% moisture whereas the cathode measurements were performed in air.

The contact resistances and volume resistances relative to the silver area in contact with the cathode are given in Fig. 5 for setups (a)–(c) shown in Fig. 4.

In the first 500 hours of operation, the area-related volume resistances drop to a value of 14–15 mΩ cm^2 on the cathode side. The resistance value of the specimen without any silver mesh between the cathode and the

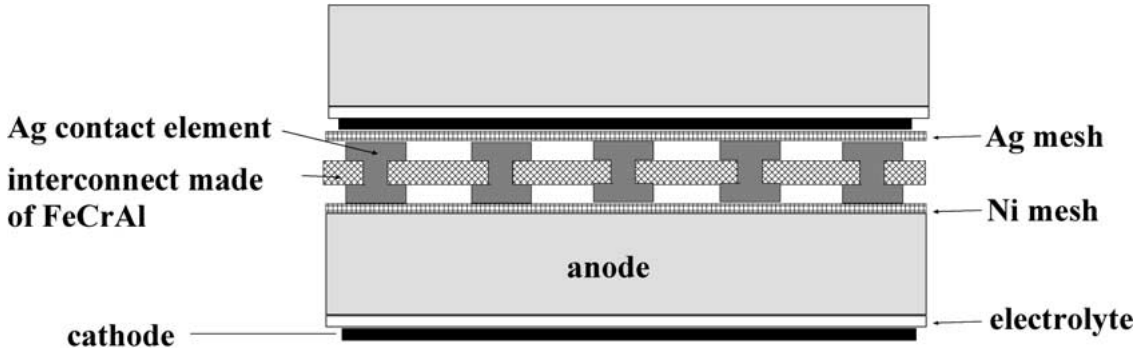

Figure 3 Contacting of a solid oxide fuel cell with silver contact elements (silver pins) and a silver mesh.

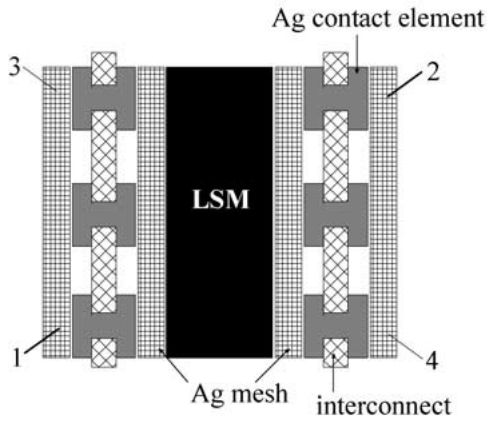

(a) Contact resistance of the Ag contact elements with lanthanum strontium manganite cathode and Ag mesh.

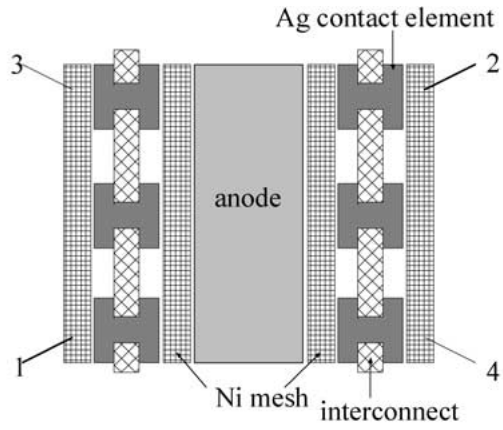

(b) Contact resistance of the Ag contact elements with Ni/ZrO_2 anode and Ni mesh.

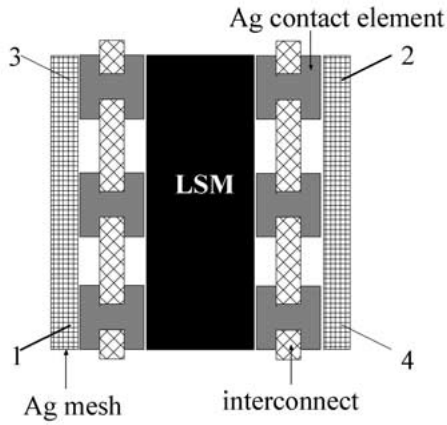

(c) Contact resistance of the Ag contact elements with lanthanum strontium manganite cathode.

1-2 contact for voltage
3-4 contact for current

Figure 4 Different measuring assemblies for contact resistance measurements at 800 °C.

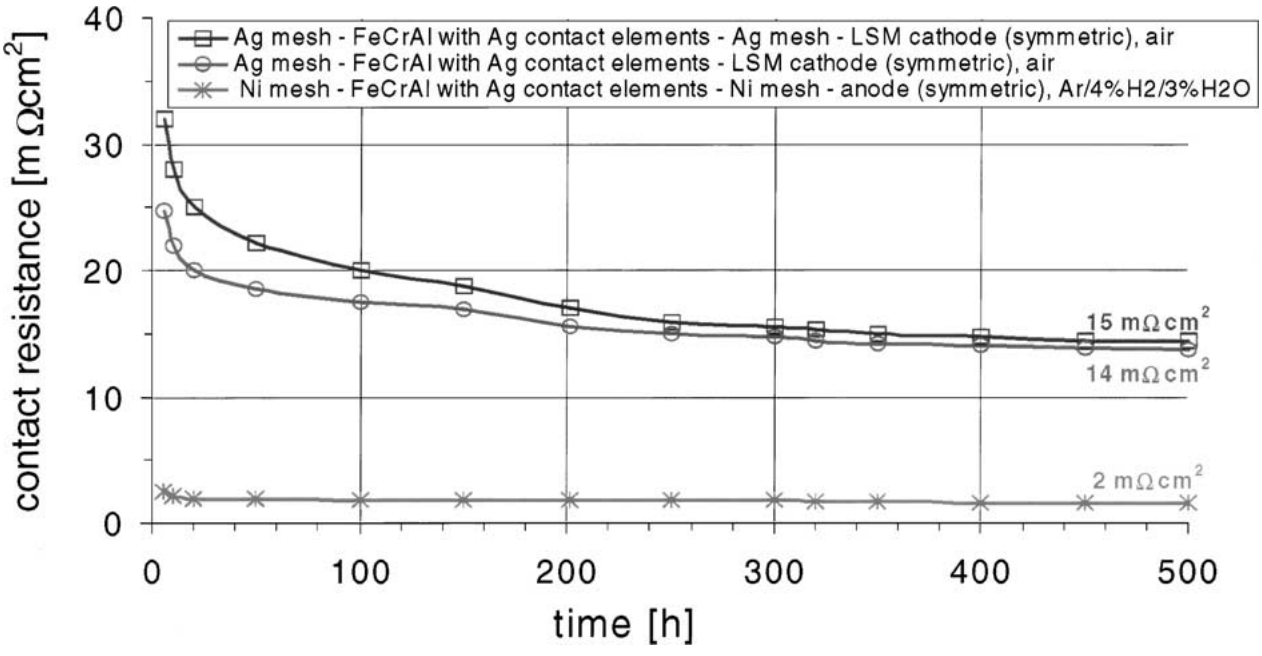

Figure 5 Contact resistances of experimental setups (a) to (c) in Fig. 4.

silver rivet heads is slightly lower. If contacting of the cathode is to be performed without any silver mesh, merely via the silver rivet heads, then the electronic current lead resistance must be taken into consideration in designing the interconnect. This resistance results from the electronic current conduction path from the reaction zone at the electrode (active electrode area) along the electrode area up to the contact area with the current-collecting component (inactive cell area), the silver pin. According to Landes [4], the spacing L of the silver pins must not exceed a critical value otherwise the ohmic resistance of the cell will become too great due to the current conduction at the interconnect. For silver pins with a head diameter of 0.3 cm, L should be $\leq$1 cm for a 50 μm-thick cathode with a specific electrical conductivity of 140 S/cm. On the anode side, a relatively constant value of 2 mΩ cm^2 is established at 800 °C after a short operating time in Ar/4 vol.% H_2/3 vol.% H_2O.

Metallic standard interconnect materials display disadvantages, above all in their corrosion resistance. The electrical conductivity between the electrodes and the interconnect is reduced by the formation of nonconducting oxide layers on their surface. This effect has, in particular, been observed on the cathode side exposed to atmospheric oxygen. Steels with a high chromium content are frequently used as interconnect materials, on whose surface a Cr_2O_3 layer is formed during operation [5]. Under operating conditions, $CrO_x(OH)_y$ vaporized out of this layer leads to a rapid deterioration of the electrochemical properties of the cathode [6].

During the 1960s the properties of Ag were investigated for use as cathode material and current collectors for SOFC systems. Other cathode materials were eventually developed due to the high volatility at 1000°C and the large thermal expansion coefficient of silver [7]. Working temperatures lower then 800°C make silver attractive again as a good conducting material.

The silver contact pins have the advantage that at an operating temperature of 800 °C they conduct current well both under reducing and also under oxidizing conditions with long-term stability since they do not form any insulating corrosion products at the silver surface which would increase the contact resistance so that the metal's good conductivity is retained. A further advantage is that the FeCrAl alloy used as a carrier foil for the silver contact elements forms a dense aluminium oxide layer several micrometres in thickness under operating conditions, largely preventing the vaporization of chromium oxide species. The vaporization behaviour of silver described in the literature, above all in an air atmosphere, prevents the use of higher temperatures for longer hold times under operating conditions [8].

3.3. He leak tests

He leak tests at room temperature and a differential pressure of 100 mbar on square plates with an edge length of 50 mm and 16 silver pins have shown that after the pressing process leak rates of $\leq 2 \times 10^{-9}$ mbar$\cdot 1 \cdot s^{-1} \cdot cm^{-2}$ are present. After being heated to 800 °C and subsequently cooled, the contact elements with additional soldering displayed the same leak rate indicating the gastightness of the joint. After a heating and cooling process at room temperature, the contact elements without additional soldering had He leak rates of 8×10^{-4} mbar $\cdot 1 \cdot s^{-1} \cdot cm^{-2}$. During the heating process, the pressed silver cannot expand uniformly in all directions thus resulting in contraction and untightnesses during subsequent cooling of the silver due to the high thermal expansion coefficient of $\alpha = 18.9 \times 10^{-6}$ K^{-1} [3].

3.4. Vaporization of silver meshes—Experimental

When silver is used as contact material, differently strong vaporizations are to be expected under operating conditions as a function of the operating temperature. The silver vaporization rate greatly depends on the surrounding atmosphere, on the gas velocity and on the specimen geometry and specimen surface. In order to determine the vaporization rate under SOFC operating conditions, three fine-silver meshes (99.99% Ag) were exposed for up to 554 and 1065 hours at temperatures between 690 °C and 800 °C (see Table I). The gas stream for exposure was about 3 l/min with a furnace pipe cross-section of 5.5 cm^2. This gas flow velocity was selected to represent approximately the order of magnitude of an SOFC stack under operating conditions.

The time-dependent mass loss in air and Ar/4 vol.% H_2/3 vol.% H_2O, from which the vaporization rates were determined, is shown in Fig. 6 and Table II. If these

TABLE II Vaporization rates and maximum mass loss after 40,000 h

mesh	temperature [°C] /atmosphere	vaporization rate [μg cm^{-2} h^{-1}]	max. mass loss after 40000 h for flushing with gas[wt.%]
1	690/air	0.094	2.16
2	790/air	1.29	28.70
3	800/Ar/H_2/H_2O	0.161	2.33

TABLE I Dimensions of the silver meshes and experimental conditions

mesh	temperature [°C] atmosphere	wire diameter [mm]	mesh width [mm]	initial weight [g]	mesh surface [cm^2]	gas volume flow (with 5.5 cm^2 pipe cross-section) [l/min]
1	690/air	0.35	0.9	6.5709	35.76	3.0
2	790/air	0.35	0.9	6.7391	36.68	3.0
3	800/Ar/4 vol.%H_2/ 3 vol.%H_2O	0.35	0.9	5.6212	30.59	3.0

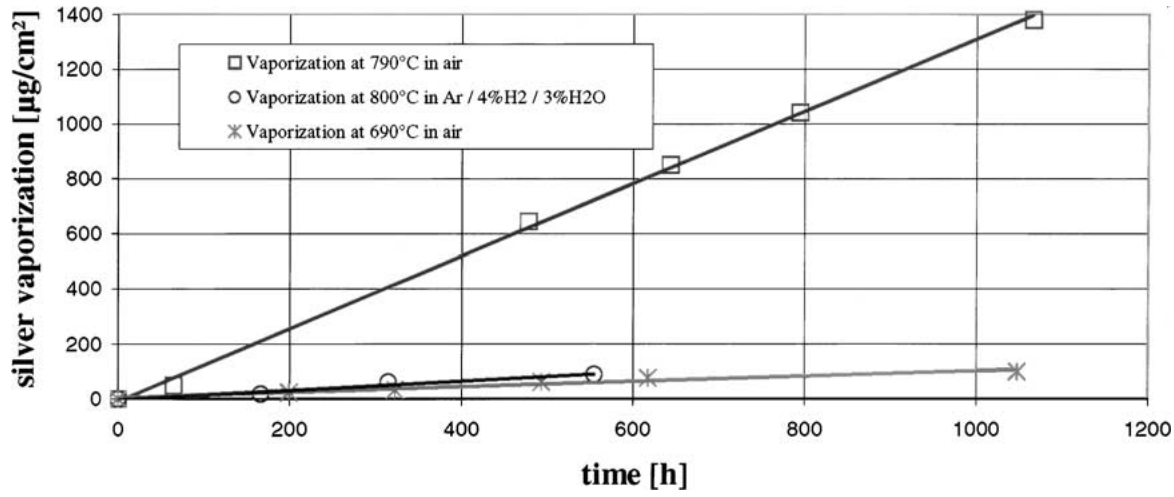

Figure 6 Vaporization rates of silver in air and Ar/4 vol.% H_2/3 vol.% H_2O.

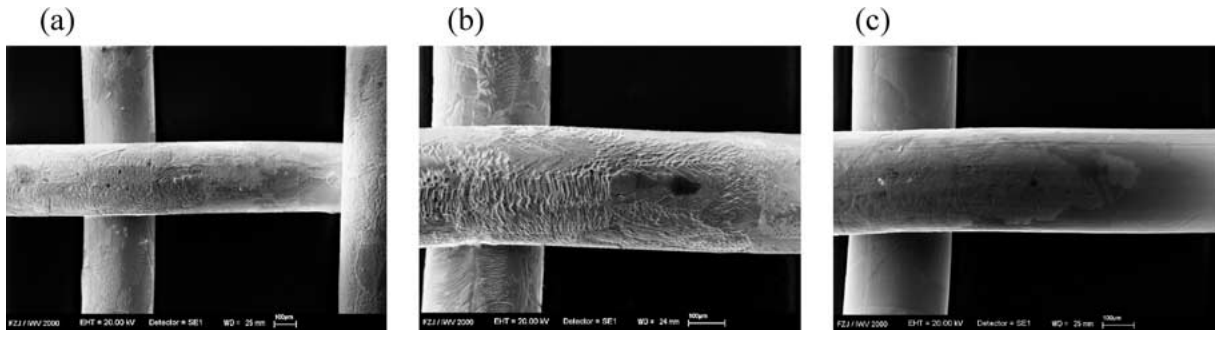

Figure 7 SEM low-power photographs of silver-mesh surfaces (99.9% Ag) after 1048 h at 690 °C under air atmosphere (a), after 1065 h at 790 °C under air atmosphere (b) and after 554 h at 800 °C under Ar/4 vol.% H_2/3 vol.% H_2O (c).

data are extrapolated to an operating period of 40,000 h required for the SOFC, a mass loss of approx. 2 wt% is obtained at an operating temperature of 690 °C in air (s. Table II). This value corresponds approximately to the mass loss of silver at 800 °C in Ar/4 vol.% H_2/3 vol.% H_2O atmosphere. The mass loss of the silver mesh examined is much higher in air at 800 °C. The mass loss determined only applies to the silver surfaces exposed to the gas atmosphere. If silver rivets are used as the contact material, the absolute mass loss is significantly reduced below the values determined due to the small silver surfaces exposed to the gas stream.

3.5. Vaporization of silver meshes—Surface structure

Even early in the 20th century, structured surfaces were documented on temperature-controlled silver in air. In 1948 Chalmers *et al*. [9] reported that an increasing facetting of the silver surface was formed

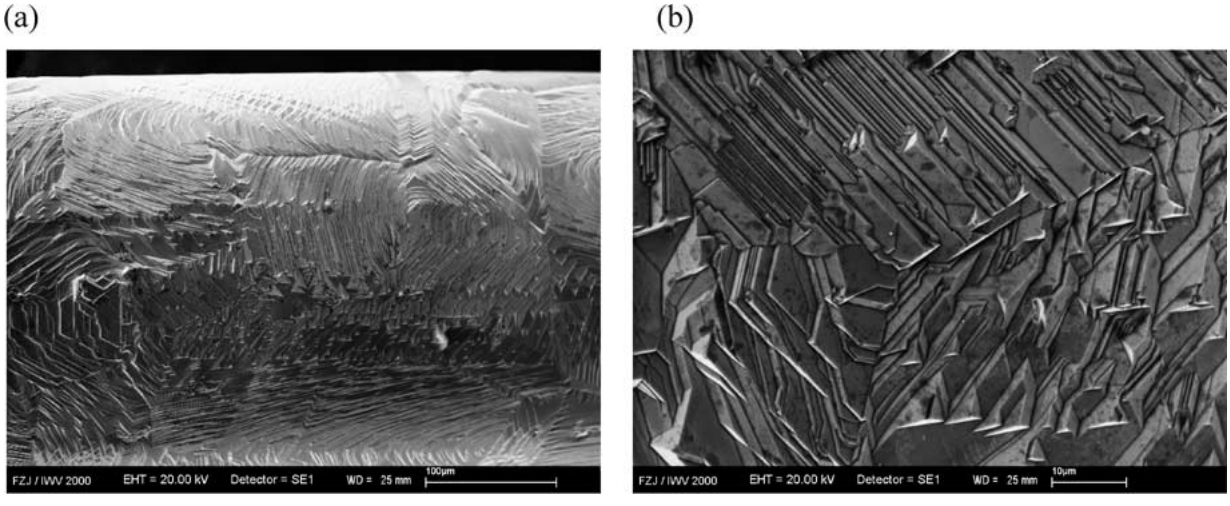

Figure 8 (a)-(b) Differently enlarged SEM photographs of silver-mesh surfaces (99.9% Ag) after 1048 h bei 690 °C under air atmosphere.

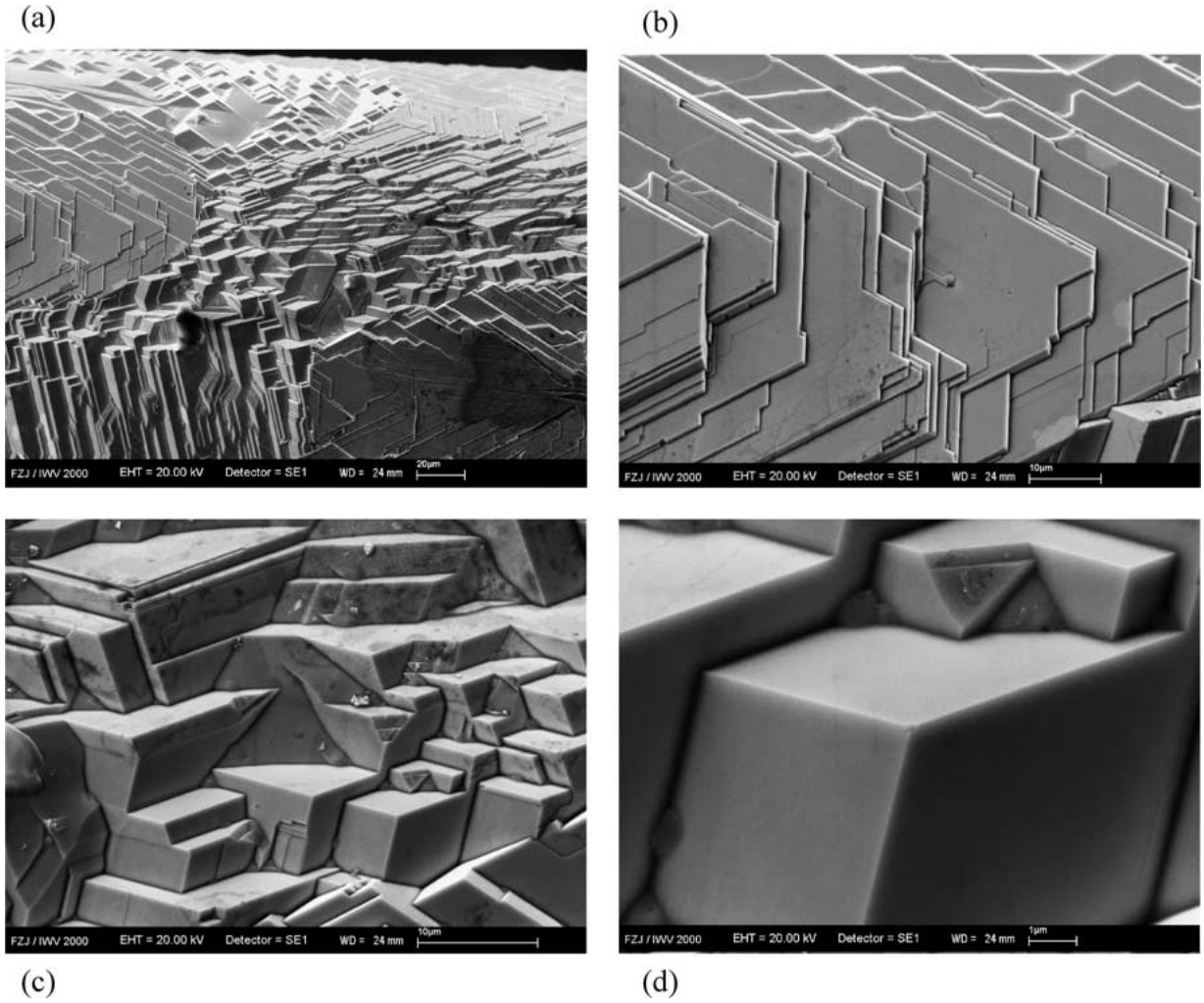

Figure 9 (a)–(d) Differently enlarged SEM photographs of silver-mesh surfaces (99.9% Ag) after 1065 h at 790 °C under air atmosphere.

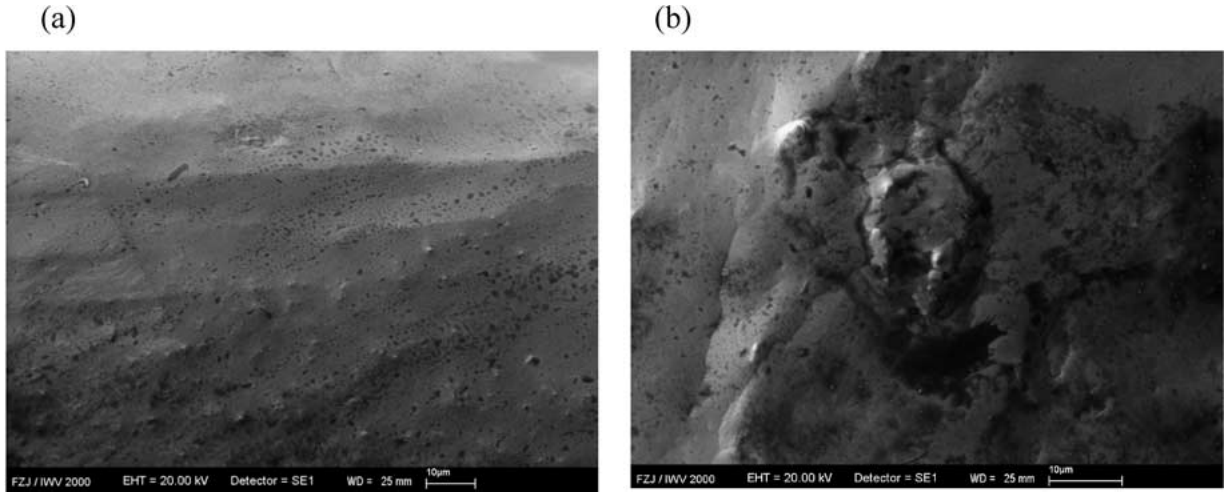

Figure 10 (a)-(b) SEM photographs of silver-mesh surfaces (99.9% Ag) after 554 h at 800 °C under Ar/4 vol.% H_2/3 vol.% H_2O.

with increasing oxygen content. Facetting does not take place in vacuum or if inert gases are used, but only grain coarsening is to be observed [10]. The surface changes on silver are attributable to thermal etching which may be attributed to two different processes. On the one hand, grain boundary growth is thermodynamically controlled. The surface is restructured via atomic diffusion so that the energetically most favourable arrangements are produced. The crystallographically random surface is restructured into low-index area elements which display a denser atomic coverage and thus a lower surface tension (equilibrium form surface). The surfaces with low surface energies such as {111} and {100} are enlarged [9, 11–13]. On the other hand, a kinetic process occurs in which silver oxide species vaporize at the surface [14]. In the temperature range below 230 °C, silver forms a passivation layer of Ag_2O in media containing oxygen. Above 230 °C, Ag_2O is

decomposed again into oxygen and elemental silver. At very high temperatures, a very thin Ag_2O layer of approx. 2–3 nm is therefore only formed [8] which, however, leads to augmented erosions at the locations with high surface energy due to vaporization and/or decomposition and forms the low-index surfaces mentioned above. In a closed system, in contrast, neither weight loss nor structural changes occur at the surface in air [14], whereas at high gas velocities the silver particles produced in the gas volume can be discharged from the system and observed as mass loss and facetting.

These effects also occur in the examined silver meshes of 99.9 wt% fine silver. In air, facetting is already perceivable after a few hours at 690 °C (see facetting after 1048 h at 690 °C in Figs 7a, 8a and b), and the facets are even more pronounced after 1065 h at 790 °C due to higher erosion caused by thermal etching (Figs 7b and 9a–d).

After 554 h in Ar/4 vol.% H_2/3 vol.% H_2O, in contrast, no structural changes of the silver at the surface are perceivable (s. Figs 7c, 10a and b). The low oxygen partial pressure in the gas mixture leads to a lower vaporization rate and surface changes in the silver mesh than in air under the same conditions and corresponds to the behaviour of silver meshes in inert gases described in the literature [10].

4. Conclusions and outlook

The first experiments showed that low contact resistance values are obtained at 800 °C for the silver pin interconnect on the cathode and anode side. In the first 500 hours of operation the contact resistance values of the specimens examined drop and this leads to the assumption that even with longer hold times no increase in these values is to be expected since no poorly conducting corrosion products are formed on silver. The vaporization rate of the silver is kept low due to the small silver surface exposed to the gas volume. First stack experiments are planned to show the assemblability and obtain first electrochemical values for a stack with the silver pin interconnect. These studies are intended to show that the new interconnect design provides an alternative to the previous design.

References

1. H. P. BUCHKREMER, U. DIEKMANN and D. STÖVER, Proceedings 2nd Eur. SOFC Forum, edited by B. Thorstensen (Switzerland, 1996) p. 221.
2. U. FLESCH, R. DAHL, R. PETERS and D. STÖVER, Proceedings 99-19 of Solid Oxide Fuel Cells (SOFC VI), edited by S. C. Singhal and M. Dokiya (1999), p. 612.
3. D. R. LIDE (ed)., "Handbook of Chemistry and Physics," 74th ed., CRC Press, Boca Raton, Ann Arbor, London, Tokyo (1994) p. 12.
4. E. LANDES, Proceedings of International Energy Agency Workshop, Hertenstein/Switzerland, June 24 to 29, 1990.
5. P. Y. HOU, K. HUANG and W. T. BAKKER, Proceedings 99-19 of Solid Oxide Fuel Cells (SOFC VI), Edited by S. C. Singhal and M. Dokiya (1999) p. 737.
6. C. GINDORF, L. SINGHEISER and K. HILPERT, Proceedings 99-19 of Solid Oxide Fuel Cells (SOFC VI), edited by S. C. Singhal and M. Dokiya (1999) p. 774.
7. C. S. TEDMON, JR, H. S. SPACIL, S. P. MITOFF, *Journal of the Electrocemical Society* **116** (1969) 1170.
8. E. FROMM and E. GEBHARDT (eds)., "Gase und Kohlenstoff in Metallen," Vol. 26 (Springer Verlag, Berlin, Heidelberg, New York, 1976) p. 678.
9. B. CHALMERS, R. KING and R. SHUTTLEWORTH, *Proceedings R. Soc. A* **193** (1948) 465.
10. M. FLYTZANI-STEPHANOPOULOS and L. D. SCHMIDT, *Progress in Surface Science* **9** (1979) 83.
11. W. SCHATT, in "Sintervorgänge" (Grundlagen, VDI Verlag, 1992) p. 34ff.
12. T.-C. WEI and J. PHILLIPS, *Advances in Catalysis* **41** (1996) 359.
13. X. BAO, G. LEHMPFUHL, G. WEINBERG, R. SCHLÖGL and G. ERTL, *Journal Chemical Society Faraday Transactions* **88**(6) (1992) 865.
14. E. D. HONDROS and A. J. W. MOORE, *Acta Metall* **8** (1960) p. 647ff.

Received 17 August 2000
and accepted 6 February 2001